

# Accepted Manuscript

On the role of synthesized hydroxylated chalcones as dual functional amyloid- $\beta$  aggregation and ferroptosis inhibitors for potential treatment of Alzheimer's disease

Lin Cong, Xiyu Dong, Yan Wang, Yulin Deng, Bo Li, Rongji Dai



PII: S0223-5234(19)30049-2

DOI: <https://doi.org/10.1016/j.ejmech.2019.01.039>

Reference: EJMECH 11046

To appear in: *European Journal of Medicinal Chemistry*

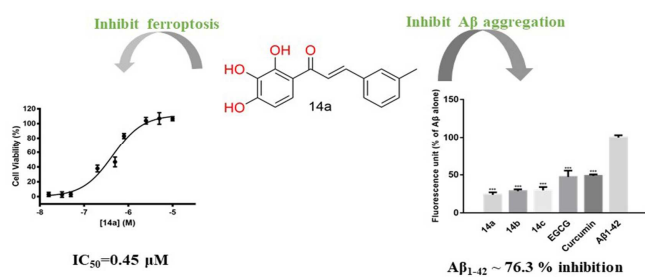
Received Date: 5 November 2018

Revised Date: 15 January 2019

Accepted Date: 15 January 2019

Please cite this article as: L. Cong, X. Dong, Y. Wang, Y. Deng, B. Li, R. Dai, On the role of synthesized hydroxylated chalcones as dual functional amyloid- $\beta$  aggregation and ferroptosis inhibitors for potential treatment of Alzheimer's disease, *European Journal of Medicinal Chemistry* (2019), doi: <https://doi.org/10.1016/j.ejmech.2019.01.039>.

This is a PDF file of an unedited manuscript that has been accepted for publication. As a service to our customers we are providing this early version of the manuscript. The manuscript will undergo copyediting, typesetting, and review of the resulting proof before it is published in its final form. Please note that during the production process errors may be discovered which could affect the content, and all legal disclaimers that apply to the journal pertain.



# On the Role of Synthesized Hydroxylated Chalcones as Dual Functional Amyloid- $\beta$ Aggregation and Ferroptosis Inhibitors for Potential Treatment of Alzheimer's Disease

Lin Cong<sup>a</sup>, Xiyu Dong<sup>b</sup>, Yan Wang<sup>a</sup>, Yulin Deng<sup>a</sup>, Bo Li<sup>a,b\*</sup>, and Rongji Dai<sup>a\*</sup>

<sup>a</sup> Beijing Key Laboratory for Separation and Analysis in Biomedicine and Pharmaceuticals, School of Life Science, Beijing Institute of Technology, Beijing, P.R. China

<sup>b</sup> Advanced Research Institute of Multidisciplinary Science, Beijing Institute of Technology, Beijing, P.R. China

## Abstract

In addition to amyloid cascade hypothesis, ferroptosis – a recently identified cell death pathway associated with the accumulation of lipid hydroperoxides – was hypothesized as one of the main forms of cell death in Alzheimer's disease. Herein, a series of hydroxylated chalcones were designed and synthesized as dual-functional inhibitors to inhibit amyloid- $\beta$  peptide ( $A\beta$ ) aggregation as well as ferroptosis simultaneously. Thioflavin-T assay indicated trihydroxy chalcones inhibited  $A\beta$  aggregation better. In human neuroblastoma SH-SY5Y cells, cytoprotective chalcones **14a-c** with three hydroxyl substituents exhibited a significant neuroprotection against  $A\beta_{1-42}$  aggregation induced toxicity. In addition, chalcones **14a-c** were found to be good inhibitors of ferroptosis induced by either pharmacological inhibition of the hydroperoxide-detoxifying enzyme Gpx4 using (*1S*, *3R*)-RSL4 or cystine/glutamate antiporter system  $X_c^-$  inhibition by erastin through lipid peroxidation inhibition mechanism. Trihydroxy chalcone **14a** was also able to completely subvert lipid peroxidation induced by  $A\beta_{1-42}$  aggregation in SH-SY5Y cells indicating that they can reduce the neurotoxicity involved with oxidative stress. Compound **14a-c** showed good ADMET properties and blood-brain barrier penetration in silico simulation software. From these data, a picture emerges wherein trihydroxy chalcones are potential candidates for the treatment of Alzheimer's disease by simultaneously inhibition of  $A\beta_{1-42}$  aggregation and ferroptosis.

Keywords: chalcone derivatives; amyloid- $\beta$  aggregation inhibition; ferroptosis inhibition; Alzheimer's Disease

## 1. Introduction

Alzheimer's disease (AD) is a chronic, progressive and irreversible neurodegenerative disease characterized by memory loss, language disorders, severe behavioral abnormalities and learning

deficits[1, 2]. Approximately 44 million people are affected by AD worldwide, and this number is expected to increase to 114 million by 2050[3]. Specific cause of AD remains unclear due to the complicated nature and diversified factors involved in the mechanism of AD, making it difficult to find an effective cure for AD. In the last three decades, U.S. Food and Drug Administration (FDA) have approved five drugs to enter the market for AD treatment. Most of them are cholinesterase inhibitors including tacrine, donepezil, rivastigmine and galantamine[4]. The other FDA approved drug to treat AD is memantine, an effective *N*-methyl-D-aspartic acid receptor (NMDA) antagonist[5]. These drugs help improve the cognitive and memory function in patients, but they can't reverse the effects of deterioration. Therefore, it seems likely that prevention of AD or halt the progress of AD at the early stage may provide reasonable strategies to help patients suffering from AD.

The most recognized hypothesis of AD is amyloid cascade hypothesis, which proposes that the aggregation and accumulation of amyloid- $\beta$  ( $A\beta$ ) in brain causes neuronal cell death[6]. One of the main features of AD is senile plaques, the product of  $A\beta$  aggregation. Amyloid- $\beta$  is generated by cleavage of the amyloid precursor protein (APP) by  $\beta$ -secretase (BACE-1) and  $\gamma$ -secretase[7]. Normally,  $A\beta$  peptide is a protein consisting of 39 to 43 amino acids, which aggregates into oligomers, protofibrils and plaques. It is suggested that oligomers consisting of  $A\beta_{1-42}$  peptides is more neurotoxic than the other  $A\beta$  peptides[8]. This provides a therapeutic treatment for AD by directly inhibition of  $A\beta$  aggregation or secretase.

Recent research has suggested a strong interplay between Alzheimer's disease and the recently characterized cell death pathway ferroptosis[9, 10]. Ferroptosis, identified in 2012, is a form of programmed cell death which is morphologically, biochemically and genetically distinct from other cell death mechanisms such as apoptosis or autophagy[11, 12]. The features of ferroptosis include the accumulation of lipid hydroperoxides and iron dysregulation, which also exists in majority of neurodegenerative diseases[13, 14]. In recent years, ferroptosis has been revealed to be associated with neurodegeneration disease, (i.e., Alzheimer's, Huntington's, and Parkinson's diseases) [15] and it has been proved to be a specific target for treating senile dementia patients[9, 16].

The progress of AD is accompanied by oxidative stress which eventually drives neuronal cell death in the brain of AD patients[17]. Numerous studies have confirmed that oxidative stress precedes the main neuropathologic manifestation of AD and may enhance the level of disease hallmarks, such as the development of amyloid plaques[18]. With the development of the concept of ferroptosis in recent years, it is reasonable to infer that oxidative stress induces cellular ferroptosis, which drives the progression of disease[13]. The development of novel ferroptosis inhibitors are currently considered as promising treatments for neurodegenerative disease. In particular,  $A\beta$  induces lipid peroxidation leading to increased amyloidogenesis through up-regulating BACE-1[19, 20]. Accordingly, radical-trapping antioxidants that inhibit lipid peroxidation will be beneficial for the treatment of AD[21, 22].

In the past decade, many researchers have devoted their efforts to develop small molecules to treat AD by either inhibiting the aggregation of  $A\beta$  or lipid peroxidation [23, 24]. Some of the small molecules are polyphenolic natural products such as epigallocatechin gallate (EGCG **1**), resveratrol (**2**) and curcumin (**3**) (**Figure 1**), which have been shown to have neuroprotective effect through protecting neurons from the  $A\beta$ -induced damages or attenuating neuronal death by oxidative stress[25]. Chalcones have been proved to exhibit a variety of pharmacological

properties including antioxidant activity, anti-inflammatory, antitumor and neuroprotection activity [26, 27]. Chalcone derivatives are the main ingredients in traditional Chinese medicine, Dragon's Blood, which has been proved to be a potential therapeutic agent of neurodegenerative diseases [28, 29]. In addition, we have found that the extract of Dragon's Blood could stimulate neurogenesis and improve learning capacity in our lab (unpublished data). These results suggest that chalcone derivatives are promising candidates for the prevention and treatment of AD, which has yet to be studied.

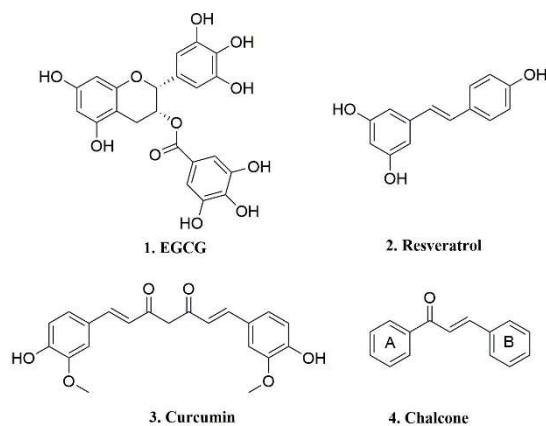


**Figure 1.** Literature reported A $\beta$  aggregation inhibitors **1-3** and chalcone

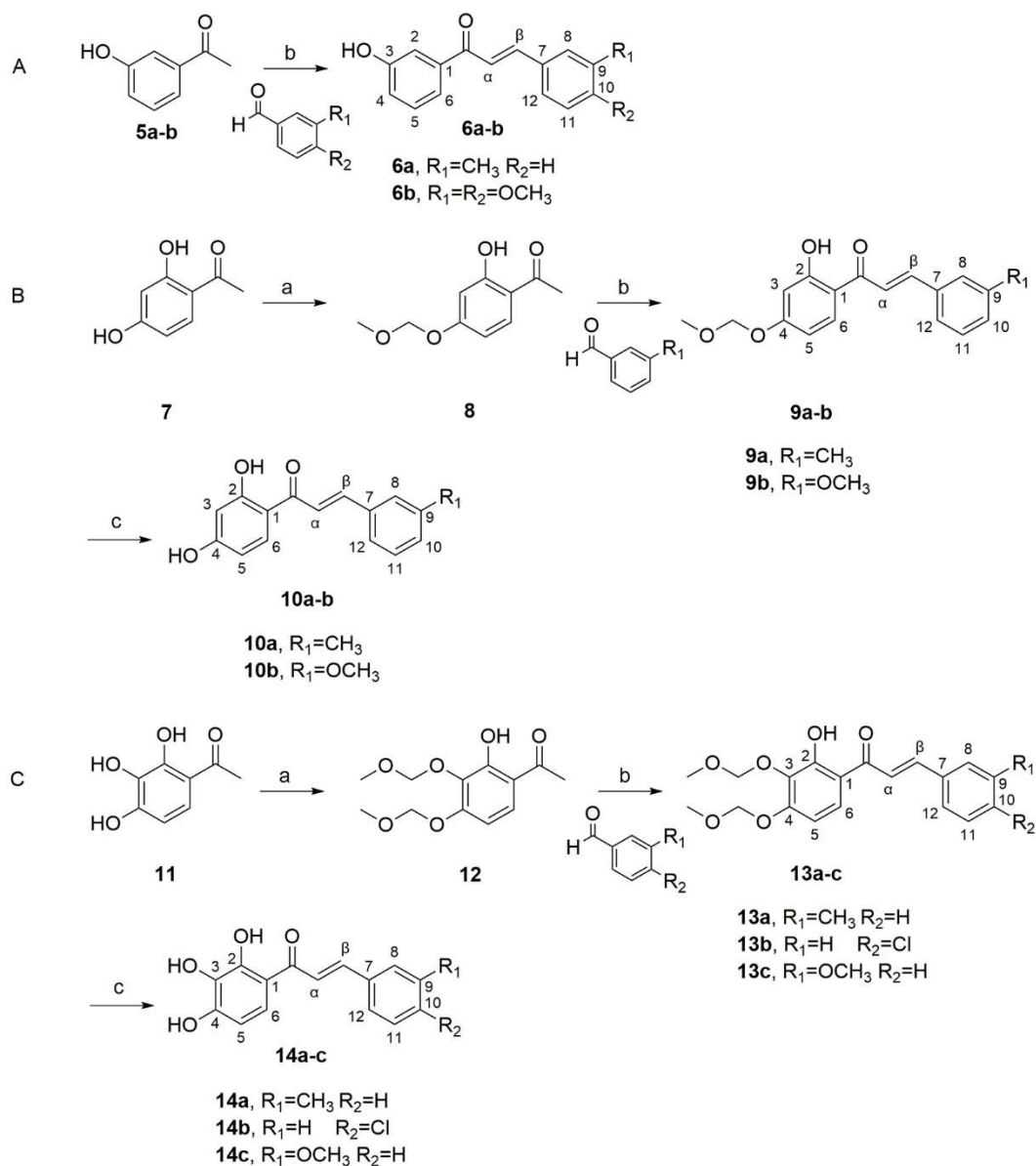
Given the essential role of A $\beta$  peptide aggregation and ferroptosis in the pathology of AD, herein, we synthesized a small library of chalcone derivatives in order to inhibit A $\beta$  peptide aggregation and ferroptosis simultaneously, which has never been reported. Their ability to inhibit A $\beta$  peptide aggregation in solution was assayed using the Thioflavin-T method [30]. The promising compounds were studied in human SH-SY5Y neuroblastoma cell lines for their anti-A $\beta$  aggregation activity and cytotoxicity property. Their ferroptosis inhibition activity was also assayed in cells. The preferential compounds have shown better drug-like properties than the lead compound EGCG and Curcumin in virtual simulation, which supports their potential to pass through blood-brain barrier and perform better *in vivo*. To the best of our knowledge, it is for the first time that the concept of inhibition ferroptosis and A $\beta$  aggregation simultaneously is brought into the molecular design for the treatment of AD. Compared to other lead compounds, we expect that these hydroxylated chalcone derivatives provide better cytoprotection of neurons for AD treatment in animal models in the near future.

## 2. Result and Discussion

### 2.1 Synthesis of chalcone derivatives

We focused on a series of chalcone derivatives **6a-b**, **10a-c**, **13a-c** and **14a-c** as the targeted dual-functional compounds to inhibit A $\beta$  aggregation and ferroptosis. The synthetic routes are shown in **Scheme 1**. The targeted compounds **6a-b** in **Scheme 1 (A)** with one hydroxyl substitution group were directly obtained from the corresponding acetophenones and benzaldehydes through the Claisen-Schmidt condensation reaction [31]. The above-described reaction was performed in 10 % KOH aqueous solution with good yields. To afford chalcones with more hydroxyl groups (**Scheme 1 (B)** and **(C)**), the hydroxyl groups were protected first by reaction with methoxymethyl chloride before reaction with the corresponding benzaldehyde

derivatives[32]. Methoxymethoxy (MOMO)-protected acetophenones (**8** and **12**) were then reacted with the corresponding benzaldehydes in ethanol to obtain the desired compounds (**9a-b** and **13a-c**). Deprotection of the MOMO group was performed using 10 % HCl in refluxing methanol to yield the targeted chalcones with two or three hydroxyl groups with good yields (**10a-b** and **14a-c**). These chalcones are stable at room temperature.



**Scheme 1.** Synthesis of chalcones **6a-b**, **10a-b**, **13a-c** and **14a-c**. Reaction conditions: (a)  $\text{CH}_3\text{OCH}_2\text{Cl}$ ,  $\text{K}_2\text{CO}_3$ , acetone, reflux, 4 h; (b) 10 % KOH aqueous, ethanol, rt, 48-96 h; (c) 10 % HCl, methanol, reflux, 20-40 min.

## 2.2 Inhibition of self-mediated $\text{A}\beta_{1-42}$ aggregation

Amyloid- $\beta$  aggregation is one of the prominent pathological features of Alzheimer's Disease. The amyloid hypothesis suggests that accumulation of aggregated  $\text{A}\beta$  in brain causes neuronal cell

death [33]. Effectively inhibition of A $\beta$  aggregation plays key role in relieving and retarding the symptom of Alzheimer's Disease. With the synthesized chalcones **6a-b**, **10a-b**, **13a-c** and **14a-c** in hands, their ability to inhibit A $\beta$  aggregation in solution was first assayed using the thioflavin-T (ThT) fluorescence method wherein EGCG and curcumin were used as reference standards[25]. ThT is a benzothiazole salt which is widely used to visualize and quantify the presence of misfolded A $\beta$  protein aggregates. When ThT binds to  $\beta$ -rich structures, such as those in A $\beta$  aggregates, it displays enhanced fluorescence ( $\lambda_{ex}$ =440 nm;  $\lambda_{em}$ =485 nm).

Fluorescence of the aqueous solution of A $\beta$  peptide in the presence and absence of the tested chalcones at 25  $\mu$ M was monitored. Inhibitory activities shown as the percent of fluorescence compared to untreated samples are summarized in **Figure 2**. Compounds **14a-c** with three hydroxyl substitutions in ring A exhibited higher inhibitory activity against A $\beta$  aggregation, with percentages of inhibition ranging from 76.3 % to 70.3 %, compared to EGCG at 52.9 % and curcumin at 51.4 %, respectively. We also examined the inhibitory activities of MOMO-protected chalcones **13a-c** to highlight the importance of additional hydroxyl groups in chalcones. Results indicated that **13a-c** could barely inhibit A $\beta$  aggregation with only 16.4 % inhibition or less, which indicated the key role of three hydroxyl groups in ring A. Compounds **10a-b** with two hydroxyl substitutions exhibited a tiny better inhibition potency (with 27.2 % and 19 % inhibition, respectively) than compounds **6a-b** having only one hydroxyl substitution. In summary, the A $\beta$  aggregation inhibitory activities of compounds we studied follow the trend **14a-c** > **10a-b** > **6a-b**  $\approx$  **13a-c**, which is consistent with the decreasing number of hydroxyls in chalcones.

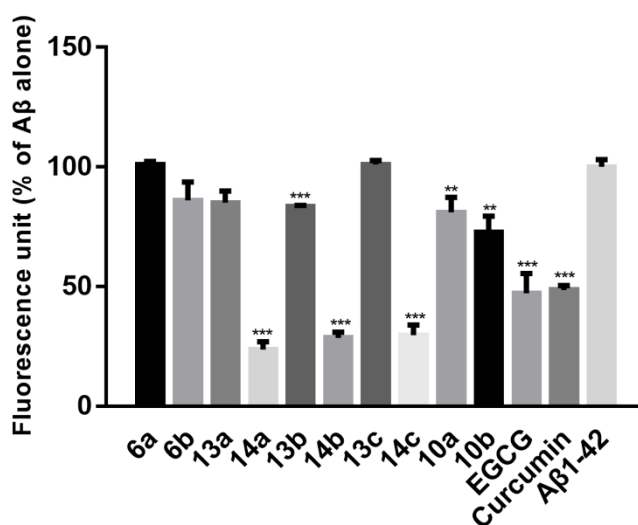


**Figure 2.** Inhibition activities of compounds on self-mediated A $\beta_{1-42}$  aggregation tested using ThT at 1:1 ratio with compounds (25  $\mu$ M) at 37 °C for 2 days. The extent of aggregation is shown as a percentage of the untreated A $\beta_{1-42}$  control. Data are reported as the mean  $\pm$  SD of at least three independent experiments, (\*\*)  $p < 0.01$ , (\*\*\*)  $p < 0.001$  vs A $\beta_{1-42}$  group; EGCG and curcumin were assayed as positive controls.

Hydrophobicity,  $\pi$ -stacking and hydrogen bonding interactions are all important factors for the anti-A $\beta$  aggregation activities[34, 35]. Coplanarity of aromatic rings and rigid planar structure also attribute to intercalate with A $\beta$  peptides[36]. We assumed that two aromatic rings and one hydrogen bond acceptor carbonyl group in chalcones provided their potency to inhibit A $\beta$  peptide aggregation. Aromatic rings in chalcones could provide hydrophobic and  $\pi$ -stacking interactions

with A $\beta$  peptides. The hydroxyl groups in ring A and carbonyl groups between two benzene rings also provide hydrogen bonding interactions between the compounds and A $\beta$  peptides. Our results with ThT fluorescent probes supported that hydrogen bonding between the compounds and A $\beta$  peptide is key in the inhibitory ability. More hydroxyl groups in chalcones provide additional hydrogen bonding donor positions, resulting in enhanced inhibition.

### 2.3 Neuronal cell protection activities

To transit results to cellular models, we further examined whether chalcone derivatives could protect cells from A $\beta_{1-42}$ -induced toxicity in SH-SY5Y cells. EGCG and curcumin were again used as reference compounds. A $\beta_{1-42}$  (10  $\mu$ M) was added to the growth medium and incubated with SH-SY5Y cells for 2 days. As indicated in **Figure 3A**, cell viability was reduced to 60.4 % compared to untreated cells upon treatment with A $\beta$  peptide. Chalcone derivatives **10a-b**, **13a-c** and **14a-c** at 20  $\mu$ M and 10  $\mu$ M (**6a-b** was excluded due to their little activity shown in ThT assays) were added to the medium for 4 h prior to the addition of A $\beta_{1-42}$ . Cell viability results indicated that compounds **14a-c** exhibited better inhibition of A $\beta$  aggregation than curcumin and EGCG (76.0 % and 92.5 %, respectively), which protect neural cells almost completely from A $\beta_{1-42}$ -induced toxicity at 10  $\mu$ M (106.2 % ~ 96.5 %). Compounds **14a-c** provided much better protection than other compounds, which were in line with the results of ThT experiments. Given the foregoing results, it is concluded that compounds **14a-c** protected neural cells from A $\beta_{1-42}$ -induced cytotoxicity by inhibiting the aggregation of A $\beta_{1-42}$ . Compared to **14a-c**, compounds **13a-c** with three MOMO-protected hydroxyl groups maintained only 72.0 % - 84.9 % cell viability at 10  $\mu$ M, indicating the importance of hydroxyl groups as hydrogen bonding donors in the inhibition activities. Treatment of SH-SY5Y cells with compounds **10a-b** provided less neuroprotective activities compared to **14a-c** with three hydroxyl groups, supporting the ThT results.

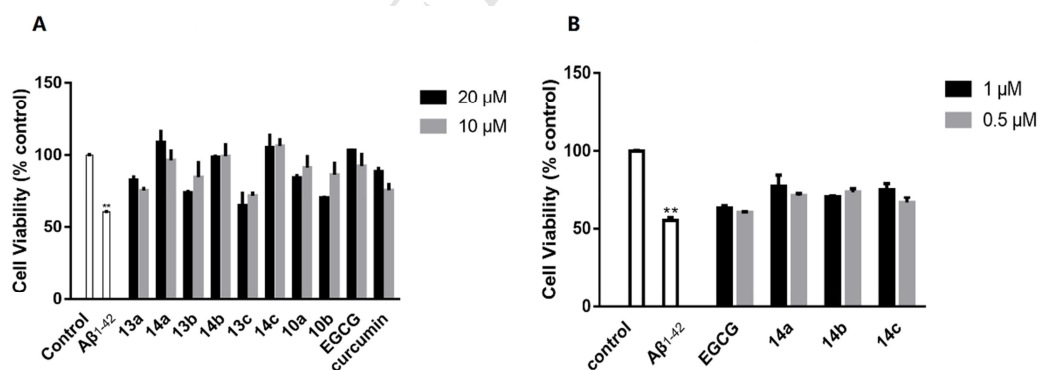


**Figure 3.** Neuroprotection of selected compounds at different concentrations (range 20-0.5  $\mu$ M) against A $\beta_{1-42}$ -induced toxicity with 48 h incubation. The results are reported as a percentage of vehicle-treated cells. Values are shown as the mean  $\pm$  SD of at least three independent experiments, (\*\*)  $p < 0.01$  vs vehicle-treated cells group; EGCG and curcumin were assayed as positive controls.

Since compounds **14a-c** could completely protect neural cells from A $\beta_{1-42}$ -induced toxicity at 10  $\mu$ M, we tried to examine the protective activities of **14a-c** at lower concentrations. Compounds **14a-c** at 1  $\mu$ M showed a moderate protection (with cell viability at 77.5 % ~ 70.8 %) compared to

$A\beta_{1-42}$  treated group (with cell viability at 55.1 %), which was better than EGCG (with cell viability at 63.0 %). When the concentration of compounds **14a-c** was decreased to 0.5  $\mu\text{M}$ , the protective effect declined slightly (with cell viability at 66.7 % ~ 73.8 %). However, cell viability of cells treated with EGCG at the same concentration was only 60.1 % (**Figure 3B**). Micrographs of cells demonstrated that compounds **14a-c** at 1  $\mu\text{M}$  indeed protected neural cells from  $A\beta_{1-42}$ -induced cytotoxicity (**Figure 4**). Cells treated with  $A\beta_{1-42}$  peptide tended to aggregate which indicated that  $A\beta_{1-42}$  peptide aggregation induced cytotoxicity (**Figure 4B**). Cells treated with  $A\beta$  peptide but in the presence of compounds **14a-c** protected cells from aggregation (**Figure 4C, D, E**).

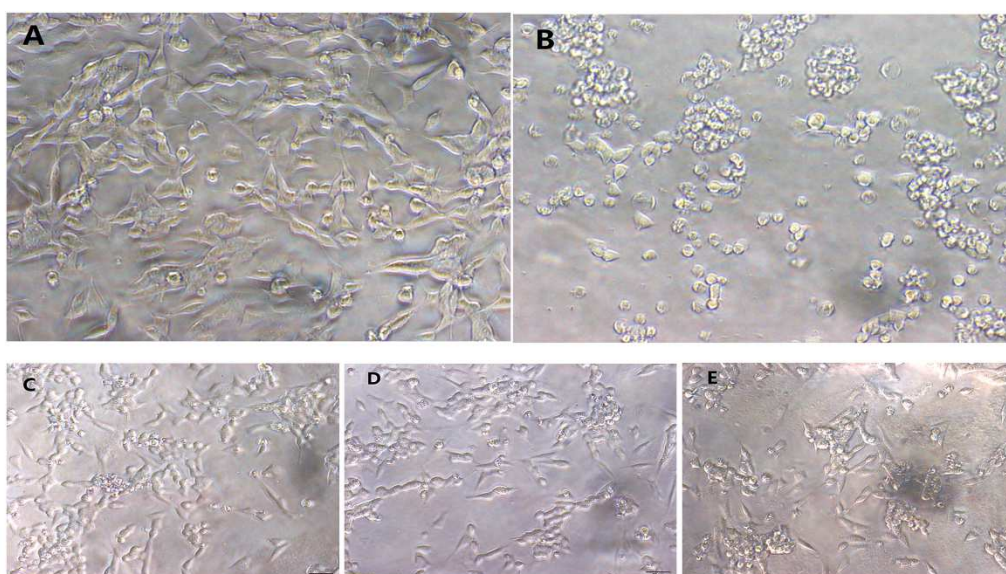


**Figure 4.** Representative micrographs of cells incubated with  $A\beta_{1-42}$  alone or with both  $A\beta_{1-42}$  (10  $\mu\text{M}$ ) and selected compounds (1  $\mu\text{M}$ ): (A) Vehicle, (B)  $A\beta_{1-42}$ , (C)  $A\beta_{1-42}$  and **14a**, (D)  $A\beta_{1-42}$  and **14b**, (E)  $A\beta_{1-42}$  and **14c**.

To further investigate neurotoxicity of chalcones, cell viabilities of human neuroblastoma SH-SY5Y cells exposed to each of compounds for 24 h at 40  $\mu\text{M}$  or 10  $\mu\text{M}$  were examined using the MTS assay. To reference the cytotoxicity of chalcones, doxorubicin was chosen as an anticancer drug which exhibited higher cytotoxicity at 40  $\mu\text{M}$  and 10  $\mu\text{M}$  with cell viability at 37.3 % and 36.6 %, respectively [37]. As shown in **Figure 5**, mono-hydroxylated **6a** had little toxicity at both 40  $\mu\text{M}$  or 10  $\mu\text{M}$ , with cell viability at 73.6 % ~ 77.4 %. All the rest of tested compounds did not exhibit observed cytotoxic effect.

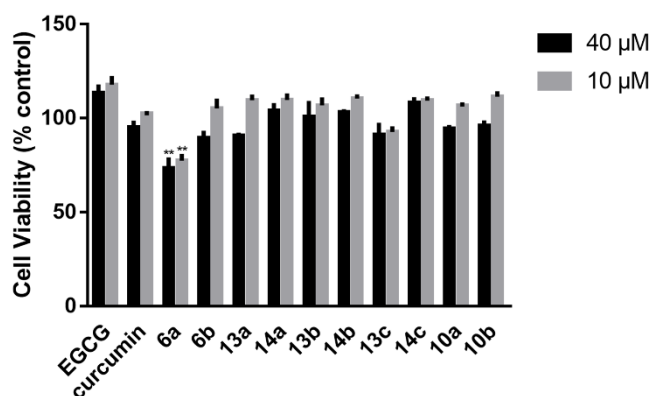


**Figure 5.** Cytotoxicity of selected compounds at different concentrations (40  $\mu\text{M}$  and 10  $\mu\text{M}$ ) with 24 h incubation. The results are reported as a percentage of control cells. Values are shown as the mean  $\pm$  SD of at least three independent experiments, (\*\*)  $p < 0.01$  vs vehicle-treated cells group; EGCG and curcumin were assayed as positive controls.

Although it has been shown that chalcones with three hydroxyl groups could effectively inhibit  $\text{A}\beta$  peptides aggregation, on the other hand, three hydroxyl groups may render the compound more difficult to pass through BBB and enter into the brain of patients[38, 39]. We used the ADMET Tool of DS to predict the ability of the designed compounds to penetrate BBB[40]. As shown in **Table 1**, compared to the lead compounds EGCG and curcumin, level of BBB penetration of most designed chalcones ranged from medium to high, which means the Brain-Blood ratio was between 5:1 and 0.3:1. In addition, all the designed compounds satisfy Lipinski and Veber's rule, indicating that they fulfill the drug-like necessity.

**Table 1.** Physical properties and ADMET prediction of the selected compounds.

Compound	MW <sup>a</sup>	ClogP <sup>a</sup>	HBA <sup>a</sup>	HBD <sup>a</sup>	PSA <sup>a</sup>	Absorption Level <sup>b</sup>	Solubility Level <sup>b</sup>	BBB Level <sup>b</sup>
EGCG	458.372	3.097	11	8	197.36	3	1	4
Curcumin	368.38	3.554	6	2	93.06	0	3	3
<b>6a</b>	238.281	3.946	2	1	37.29	0	2	1
<b>6b</b>	284.307	3.427	4	1	55.76	0	3	1
<b>14a</b>	270.28	3.462	4	3	77.76	0	3	2
<b>13a</b>	358.385	3.616	6	1	74.22	0	3	2
<b>14b</b>	286.279	2.959	5	3	86.99	0	3	3
<b>13b</b>	374.384	3.113	7	1	83.45	0	3	2
<b>14c</b>	290.698	3.64	4	3	77.76	0	3	2
<b>13c</b>	378.804	3.794	6	1	74.22	0	2	2
<b>10a</b>	254.281	3.704	3	2	57.53	0	3	1
<b>10b</b>	270.28	3.201	4	2	66.76	0	3	2

a MW: molecular weight; Clog P: calculated logarithm of the octanol-water partition coefficient; HBA: hydrogen-bond acceptor atoms; HBD: hydrogen-bond donor atoms; PSA: polar surface area;

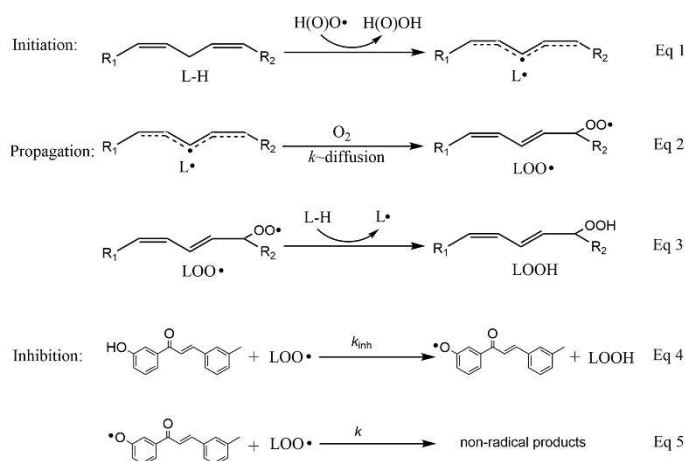
b Absorption level (0: good, 3: very poor); Solubility level (0: extremely low, 3: good); BBB level(1: high, 2:

medium, 3: low and 4: undefined);

## 2.4 Inhibition of cellular lipid peroxidation and ferroptosis

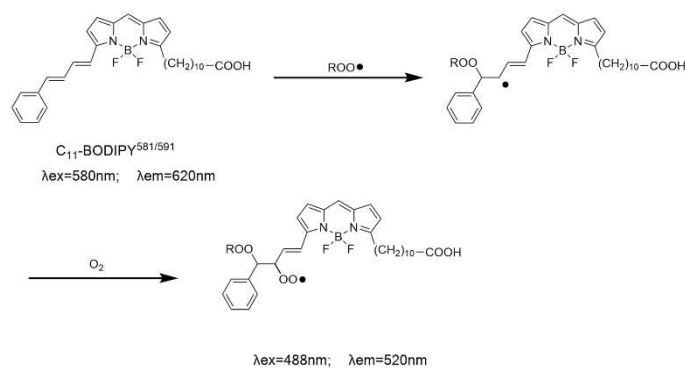
The accumulation of lipid hydroperoxides (LOOH) has long been implicated in cell death and dysfunction, initiating or deteriorating neurodegenerative disease including Alzheimer's disease[19]. However, only recently has a novel cellular death form – ferroptosis been directly linked to the accumulation of lipid peroxidation associated with neurodegenerative disease[41]. It has been recently elucidated that ferroptosis is one of the main pathogenic mechanism of AD. Effective anti-ferroptotic molecules are protective in animal models to treat neurodegenerative disease, and anti-ferroptotic iron chelator deferiprone is currently being tested in a phase 2 randomized controlled trial for AD[42].

Lipid peroxidation is a free radical chain reaction involving with initiation (**Scheme 2 Eq1**) and propagation steps (**Scheme 2 Eq 2-3**). The hydroxyl groups in chalcone derivatives could react with lipid peroxyl radicals by H-atom transfer to inhibit lipid peroxidation through the mechanism shown in **Scheme 2 Eq4-5**[43].



**Scheme 2.** Mechanism of lipid peroxidation and its inhibition by chalcone (e.g., compound **6a**)

To provide more insight on the potencies of chalcones as lipid peroxidation inhibitors, we carried out experiments to examine whether chalcones with best  $A\beta_{1-42}$  aggregation inhibitory activities **14a-c** could inhibit lipid peroxidation in cellular models. We chose compound **14a** as an example. To corroborate that  $A\beta_{1-42}$ -induced cells express higher rate of lipid peroxidation, commercial available fluorescent probe C11-BODIPY<sup>581/591</sup> was used as a lipid peroxidation indicator[44]. Upon lipid peroxidation, the fluorescence of C11-BODIPY<sup>581/591</sup> ( $\lambda_{ex} = 488 \text{ nm}$ ;  $\lambda_{em} = 525 \text{ nm}$ ) is increased (**Scheme 3**).



**Scheme 3.** The reaction of C11-BODIPY<sup>581/591</sup> with peroxyl radicals.

As shown in **Figure 6A**, incubating cells with A $\beta$ <sub>1-42</sub> (10  $\mu\text{M}$ ) for two days induced higher level of lipid peroxidation by 54.0 %. The fluorescence decreased to untreated control level when the cells were incubated with A $\beta$ <sub>1-42</sub> (10  $\mu\text{M}$ ) in the presence of compound **14a** (10  $\mu\text{M}$ ) for 48 h, indicating that increased level of lipid peroxidation induced by A $\beta$  aggregation was inhibited by compound **14a**. These results revealed that **14a** can not only inhibit the aggregation of A $\beta$ <sub>1-42</sub>, but also inhibit lipid peroxidation derived therefrom.

We further replaced A $\beta$ <sub>1-42</sub> with (1*S*,3*R*)-RSL3 to examine the ability of **14a-c** to inhibit ferroptosis – a recently recognized cell death form associated with lipid peroxidation. (1*S*,3*R*)-RSL3 stimulated cellular ferroptosis by pharmacological inhibition of the hydroperoxide-detoxifying enzyme Gpx4. The results were in agreement with the above analysis. When cells were treated with RSL3 (500 nM) for one day, the fluorescence of the sample increased indicating the level of lipid peroxidation increased compared to the untreated cells. Whereas compounds **14a-c** could reduce the level of lipid peroxidation to the normal level as untreated cells (**Figure 6B**). These results served as more direct affirmation that **14a-c** could inhibit lipid peroxidation derived from ferroptosis effectively.

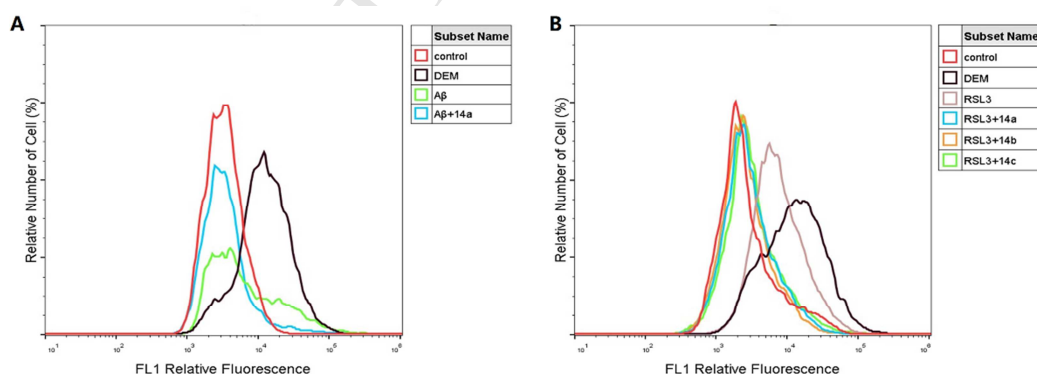


**Figure 6.** Histogram obtained from flow cytometry ( $3 \times 10^5$  cells/ml;  $\lambda_{\text{ex}} = 488$  nm,  $\lambda_{\text{em}} = 525 \pm 25$  nm; 10,000 events) following induction of oxidative stress with A $\beta$  (15  $\mu\text{M}$ ) in SH-SY5Y cells (A) or RSL3 (5  $\mu\text{M}$ ) in HEK-293 cells (B) grown in media containing **14a-c** (10  $\mu\text{M}$ ) for 24–48 h. Cells treated with Vehicle were used as positive control (red).

Given that chalcones **14a-c** with three hydroxyl groups could inhibit lipid peroxidation revealed by flow cytometry, we assayed their inhibitory activity of ferroptosis in cellular models thoroughly.

Cellular ferroptosis was induced in HEK-293 cells by either pharmacological inhibition of glutathione peroxidase 4 (Gpx4) using (1*S*,3*R*)-RSL3 or glutathione (GSH) depletion by the system xc<sup>-</sup> inhibitor erastin[45, 46]. The results shown in **Table 2** demonstrated that compounds **14a-c** were effective inhibitors of (1*S*,3*R*)-RSL3 induced ferroptosis. In contrast, EGCG didn't show any ferroptosis inhibitory activity at concentrations up to 20 μM. Compound **14a** (IC<sub>50</sub> = 0.45 μM) exhibited the highest inhibitory activity than **14b** and **14c** (IC<sub>50</sub> = 1.77 μM ~ 0.86 μM). Compounds **14a-c** also inhibited erastin-induced ferroptosis with IC<sub>50</sub> at 3.15 μM ~ 3.88 μM. These results indicated that **14a** is a better dual-functional inhibitor for ferroptosis and Aβ aggregation simultaneously associated with AD.

**Table 2.** Inhibition of (1*S*,3*R*)-RSL3 and erastin induced ferroptosis by the selected compounds<sup>a</sup>.

Compounds	Inhibition of ferroptosis	
	IC <sub>50</sub> ± SD (μM) for (1 <i>S</i> ,3 <i>R</i> )-RSL3 induced ferroptosis <sup>b</sup>	IC <sub>50</sub> ± SD (μM) for erastin induced ferroptosis <sup>b</sup>
<b>14a</b>	0.45 ± 0.05	3.81 ± 0.11
<b>14b</b>	1.77 ± 0.01	3.88 ± 0.15
<b>14c</b>	0.86 ± 0.01	3.15 ± 0.08
EGCG	N <sup>c</sup>	N <sup>c</sup>

<sup>a</sup>Cell viabilities were determined 24 h post induction by MTS assay.

<sup>b</sup>IC<sub>50</sub>: 50 % inhibition concentration. Results are shown as the mean of at least three experiments.

<sup>c</sup>N means no active. Compounds defined “not active” meant that percent inhibition was less than 10 % at 20 μM.

### 3. Conclusions

Herein we have presented a series of chalcone derivatives functionalized with various number of hydroxyl groups in ring A and different substitutions in ring B, which were synthesized in an expeditious manner in order to achieve the first time reported candidates for the treatment of AD by inhibition of Aβ aggregation and ferroptosis simultaneously. We determined how systematic changes in the number of hydroxyl groups and substitution groups impact their inhibitory activities of Aβ aggregation and ferroptosis. It was found that chalcones with different number of hydroxyl substitutions have a quite different inhibitory activities of Aβ<sub>1-42</sub> aggregation, with more hydroxyl groups providing increasing activities. Chalcone derivatives **14a-c** exhibited low toxicity and better neuroprotection against Aβ<sub>1-42</sub>-induced neurotoxicity than the lead compounds EGCG and curcumin in the SH-SY5Y cellular assays. In addition, they also displayed potent anti-ferroptotic cell death activities by lipid peroxidation inhibition in cellular assays. Among them, compound **14a** with three hydroxyl groups in ring A and methyl group in ring B prevented ferroptosis with the lowest IC<sub>50</sub> values. Due to the predicted good BBB permeability, we expect that compound **14a** is a potent molecule for further evaluation *in vivo* in the near future. Given the recent hypothesis that ferroptosis is the main form of cell death in Alzheimer's disease, our results may indicate a novel idea using dual functional inhibitors for Aβ peptide aggregation and ferroptosis in molecular design.

### 4. Experimental Section

#### Materials

Reagents and solvents were purchased from commercial sources and used as received.

Reactions were monitored by thin layer chromatography on precoated silica gel GF254 plates under 254 nm UV light. Column chromatography was performed with silica gel (200-300 mesh).  $^1\text{H}$  and  $^{13}\text{C}$  nuclear magnetic resonance (NMR) spectra were recorded using Bruker Avance III 400 spectrometer at 700 MHz, 400 MHz and 175 MHz with tetramethylsilane (TMS) as the internal standard at Analysis & Testing Center of Beijing Institute of Technology. High resolution mass spectra (HRMS) were obtained with an Agilent 6520 LCMS-Q-TOF mass spectrometer at Analysis & Testing Center of Beijing Institute of Technology.

#### General procedure for the synthesis of intermediates 8 and 12[32]

Hydroxyacetophenone( 1 mmol )and  $\text{K}_2\text{CO}_3$ ( 3 mmol )were added to dry acetone (30 mL). The reaction mixture was cooled on ice bath for 30 min until the solid was dissolved completely. Methoxymethyl chloride (4 mmol) was added dropwise when stirring, and the reaction mixture was subsequently refluxed for 4 h. Upon completion of the reaction as indicated by TLC, the resulting solution was cooled to room temperature and then filtered to remove the precipitated salts. Acetone was evaporated under reduced pressure and the crude product was purified by silica gel column chromatography using ethyl acetate/petroleum ether (1:5) as eluent to afford the pure product.

#### General procedure for the synthesis of intermediates 9a-b, 13a-c and chalcones 6a-b

Acetophenone (0.5 mmol) was dissolved in ethanol (20 mL), and an aqueous solution of KOH ( 10 % w/v, 10 mL ) was added. After the solid was dissolved completely, aryl aldehyde (0.6 mmol) was added to the mixture. The reaction mixture was then stirred at room temperature for 48-96 h. Upon completion of the reaction as indicated by TLC, the mixture was acidified with HCl (10 % v/v aqueous solution) to pH 7, and then extracted with 3×50 mL ethyl acetate. The combined organic layers were washed with brine, dried over  $\text{MgSO}_4$ , filtered and concentrated to yield crude product which was purified by silica gel chromatography (gradient ethyl acetate/petroleum ether from 1/10 to 1/3).

#### General procedure for the synthesis of chalcones 10a-b and 14a-c

Methoxymethoxy-protected chalcones (0.5 mmol) was added to methanol (20 mL), and HCl (10 % v/v aqueous solution, 5 mL) was added dropwise when the mixture was refluxed for 20-40 min. After cooled down to room temperature, the mixture was diluted with water (40 mL), and extracted with 3×50 mL of ethyl acetate. The product was recrystallized from ethyl acetate in petroleum ether (1:1) to yield the products as yellow solid.

#### (*E*)-1-(3-hydroxyphenyl)-3-(*m*-tolyl)prop-2-en-1-one (6a)

Synthesis was completed according to the general synthetic procedure mentioned above. The product was isolated by silica gel chromatography using ethyl acetate/petroleum ether (1:3) as yellow powder with 74.2 % yield; mp 87 – 89 °C;  $^1\text{H}$  NMR (700 MHz,  $\text{CDCl}_3$ )  $\delta$  7.82 (d,  $J$  = 15.7 Hz, 1H,  $\text{H}_\beta$ ), 7.72 (dd,  $J$  = 2.3, 1.7 Hz, 1H,  $\text{H}_2$ ), 7.59 (d,  $J$  = 7.7 Hz, 1H,  $\text{H}_6$ ), 7.52 (d,  $J$  = 15.7 Hz, 1H,  $\text{H}_\alpha$ ), 7.44 (s, 1H,  $\text{H}_8$ ), 7.43(d,  $J$  = 7.7 Hz, 1H,  $\text{H}_{12}$ ), 7.39 (t,  $J$  = 7.9 Hz, 1H,  $\text{H}_5$ ), 7.31 (t,  $J$  = 7.7 Hz, 1H,  $\text{H}_{11}$ ), 7.24 (d,  $J$  = 7.4 Hz, 1H,  $\text{H}_{10}$ ), 7.18 (dd,  $J$  = 8.1, 2.5Hz, 1H,  $\text{H}_4$ ), 2.40 (s, 3H,  $\text{CH}_3$ );

$^{13}\text{C}$  NMR (100 MHz,  $\text{CDCl}_3$ )  $\delta$  191.54, 156.76, 146.06, 139.29, 138.61, 134.54, 131.68, 129.89, 129.28, 128.83, 125.82, 121.63, 120.86, 120.77, 115.42, 21.28; HRMS (EI)  $m/z$  calcd for  $\text{C}_{16}\text{H}_{14}\text{O}_2(\text{M}^+)$  239.0994, found 239.1056.

*(E)*-1-(3,4-dimethoxyphenyl)-3-(3-hydroxyphenyl)prop-2-en-1-one (**6b**)

Synthesis was completed according to the general synthetic procedure mentioned above. The product was isolated by silica gel chromatography using ethyl acetate/petroleum ether (1:2) as yellow powder with 61.9 % yield; mp 120 – 122 °C;  $^1\text{H}$  NMR (700 MHz,  $\text{CDCl}_3$ )  $\delta$  7.75 (d,  $J$  = 15.5 Hz, 1H,  $\text{H}_\beta$ ), 7.67 (s, 1H,  $\text{H}_3$ ), 7.54 (d,  $J$  = 7.6 Hz, 1H,  $\text{H}_2$ ), 7.34 (d,  $J$  = 15.3 Hz, 1H,  $\text{H}_a$ ), 7.31 (d,  $J$  = 7.7 Hz, 1H,  $\text{H}_5$ ), 7.16 (d,  $J$  = 8.2 Hz, 1H,  $\text{H}_{12}$ ), 7.13 (d,  $J$  = 8.0 Hz, 1H,  $\text{H}_4$ ), 7.10 (s, 1H,  $\text{H}_8$ ), 6.84 (d,  $J$  = 8.3 Hz, 1H,  $\text{H}_{11}$ ), 3.89 (s, 3H,  $\text{OCH}_3$ ), 3.88 (s, 3H,  $\text{OCH}_3$ );  $^{13}\text{C}$  NMR (175 MHz,  $\text{CDCl}_3$ )  $\delta$  191.30, 156.83, 151.61, 149.18, 145.92, 139.59, 129.86, 127.69, 123.46, 120.69, 120.52, 119.80, 115.39, 111.16, 110.31, 55.99, 55.97; HRMS (EI)  $m/z$  calcd for  $\text{C}_{17}\text{H}_{16}\text{O}_4(\text{M}^+)$  285.1049, found 285.1113.

*(E)*-1-(3,5-bis(methoxymethoxy)phenyl)-3-(*m*-tolyl)prop-2-en-1-one (**9a**)

Synthesis was completed according to the general synthetic procedure mentioned above. The product was isolated by silica gel chromatography using ethyl acetate/petroleum ether (1:10) as yellow powder with 74.5 % yield; mp 78 – 80 °C;  $^1\text{H}$  NMR (400 MHz,  $\text{CDCl}_3$ )  $\delta$  13.31 (s, 1H, OH), 7.83 (d,  $J$  = 15.3 Hz, 1H,  $\text{H}_\beta$ ), 7.82 (d,  $J$  = 9.1 Hz, 1H,  $\text{H}_6$ ), 7.53 (d,  $J$  = 15.5 Hz, 1H,  $\text{H}_a$ ), 7.42 (d,  $J$  = 6.1 Hz, 2H,  $\text{H}_8$ ,  $\text{H}_{12}$ ), 7.29 (t,  $J$  = 7.8 Hz, 1H,  $\text{H}_{11}$ ), 7.22 (d,  $J$  = 7.5 Hz, 1H,  $\text{H}_{10}$ ), 6.63 (d,  $J$  = 2.4 Hz, 1H,  $\text{H}_3$ ), 6.57 (dd,  $J$  = 8.9, 2.4 Hz, 1H,  $\text{H}_5$ ), 5.20 (s, 2H,  $\text{CH}_2$ ), 3.47 (s, 3H,  $\text{OCH}_3$ ), 2.38 (s, 3H,  $\text{CH}_3$ );  $^{13}\text{C}$  NMR (175 MHz,  $\text{CDCl}_3$ )  $\delta$  192.07, 166.25, 163.66, 144.84, 138.69, 134.69, 131.64, 131.40, 129.16, 128.90, 119.97, 114.97, 108.24, 103.94, 94.03, 56.42, 21.36; HRMS (EI)  $m/z$  calcd for  $\text{C}_{20}\text{H}_{22}\text{O}_5(\text{M}^+)$  343.1467, found 343.1518.

*(E)*-1-(3,5-bis(methoxymethoxy)phenyl)-3-(4-methoxyphenyl)prop-2-en-1-one (**9b**)

Synthesis was completed according to the general synthetic procedure mentioned above. The product was isolated by silica gel chromatography using ethyl acetate/petroleum ether (1:10) as yellow powder with 64.2 % yield; mp 221 – 223 °C;  $^1\text{H}$  NMR (400 MHz,  $\text{CDCl}_3$ )  $\delta$  13.28 (s, 1H, OH), 7.81 (d,  $J$  = 15.4 Hz, 1H,  $\text{H}_\beta$ ), 7.80 (d,  $J$  = 9.0 Hz, 1H,  $\text{H}_6$ ), 7.52 (d,  $J$  = 15.4 Hz, 1H,  $\text{H}_a$ ), 7.31 (t,  $J$  = 7.9 Hz, 1H,  $\text{H}_{12}$ ), 7.23 (d,  $J$  = 7.7 Hz, 1H,  $\text{H}_8$ ), 7.12 (s, 1H,  $\text{H}_{11}$ ), 6.95 (dd,  $J$  = 8.1, 2.4 Hz, 1H,  $\text{H}_{10}$ ), 6.62 (d,  $J$  = 2.4 Hz, 1H,  $\text{H}_3$ ), 6.57 (dd,  $J$  = 8.9, 2.4 Hz, 1H,  $\text{H}_5$ ), 5.20 (s, 2H,  $\text{CH}_2$ ), 3.83 (s, 3H,  $\text{OCH}_3$ ), 3.47 (s, 3H,  $\text{OCH}_3$ );  $^{13}\text{C}$  NMR (175 MHz,  $\text{CDCl}_3$ )  $\delta$  191.97, 166.24, 163.70, 159.97, 144.51, 136.09, 131.40, 130.00, 121.17, 120.48, 116.39, 114.92, 113.68, 108.27, 103.93, 94.02, 56.42, 55.34; HRMS (EI)  $m/z$  calcd for  $\text{C}_{20}\text{H}_{22}\text{O}_6(\text{M}^+)$  359.1416, found 359.1497.

*(E)*-1-(3,5-dihydroxyphenyl)-3-(*m*-tolyl)prop-2-en-1-one (**10a**)

Synthesis was completed according to the general synthetic procedure mentioned above. The product was isolated by silica gel chromatography using ethyl acetate/petroleum ether (1:5) as yellow powder with 67.4 % yield; mp 126 – 128 °C;  $^1\text{H}$  NMR (400 MHz, MeOD)  $\delta$  7.94 (d,  $J$  = 8.9 Hz, 1H,  $\text{H}_6$ ), 7.76 (d,  $J$  = 15.5 Hz, 1H,  $\text{H}_\beta$ ), 7.70 (d,  $J$  = 15.5 Hz, 1H,  $\text{H}_a$ ), 7.49 (s, 1H,  $\text{H}_8$ ), 7.48 (d,  $J$  = 8.7 Hz, 1H,  $\text{H}_{12}$ ), 7.28 (t,  $J$  = 7.5 Hz, 1H,  $\text{H}_{11}$ ), 7.21 (d,  $J$  = 7.5 Hz, 1H,  $\text{H}_{10}$ ), 6.42 (dd,  $J$  = 8.9, 2.4 Hz, 1H,  $\text{H}_5$ ), 6.31 (d,  $J$  = 2.4 Hz, 1H,  $\text{H}_3$ ), 2.36 (s, 3H,  $\text{CH}_3$ );  $^{13}\text{C}$  NMR (175 MHz,

MeOD)  $\delta$  191.95, 166.24, 165.21, 143.97, 138.49, 134.85, 132.19, 131.03, 128.93, 128.51, 125.49, 120.13, 113.30, 107.89, 102.46, 19.95; HRMS (EI)  $m/z$  calcd for  $C_{16}H_{14}O_3(M^+)$  255.0943, found 255.1020.

*(E)*-1-(3,5-dihydroxyphenyl)-3-(4-methoxyphenyl)prop-2-en-1-one (**10b**)

Synthesis was completed according to the general synthetic procedure mentioned above. The product was isolated by silica gel chromatography using ethyl acetate/petroleum ether (1:5) as yellow powder with 73.4 % yield; mp 146 – 148 °C;  $^1H$  NMR (400 MHz, MeOD)  $\delta$  7.92 (d,  $J$  = 8.9 Hz, 1H,  $H_6$ ), 7.73 (d,  $J$  = 15.5 Hz, 1H,  $H_\beta$ ), 7.67 (d,  $J$  = 15.5 Hz, 1H,  $H_\alpha$ ), 7.32 – 7.17 (m, 3H,  $H_8$ ,  $H_{11}$ ,  $H_{12}$ ), 6.93 (dd,  $J$  = 7.8, 1.8 Hz, 1H,  $H_{10}$ ), 6.41 (dd,  $J$  = 8.9, 2.4 Hz, 1H,  $H_5$ ), 6.31 (d,  $J$  = 2.4 Hz, 1H,  $H_3$ ), 3.80 (s, 3H,  $OCH_3$ );  $^{13}C$  NMR (175 MHz, MeOD)  $\delta$  191.86, 166.22, 165.21, 160.10, 143.71, 136.22, 132.24, 129.58, 120.94, 120.58, 116.12, 113.32, 113.12, 107.91, 102.48, 54.42; HRMS (EI)  $m/z$  calcd for  $C_{16}H_{14}O_4(M^+)$  271.0892, found 271.0946.

*(E)*-1-(2-hydroxy-3,4-bis(methoxymethoxy)phenyl)-3-(*m*-tolyl)prop-2-en-1-one (**13a**)

Synthesis was completed according to the general synthetic procedure mentioned above. The product was isolated by silica gel chromatography using ethyl acetate/petroleum ether (1:7) as yellow powder with 70.7 % yield; mp 72 – 74 °C;  $^1H$  NMR (400 MHz,  $CDCl_3$ )  $\delta$  13.34 (s, 1H, OH), 7.84 (d,  $J$  = 15.5 Hz, 1H,  $H_\beta$ ), 7.65 (d,  $J$  = 9.2 Hz, 1H,  $H_6$ ), 7.53 (d,  $J$  = 15.5 Hz, 1H,  $H_\alpha$ ), 7.44 – 7.40 (m, 2H,  $H_8$ ,  $H_{12}$ ), 7.28 (t,  $J$  = 7.5 Hz, 1H,  $H_{11}$ ), 7.21 (d,  $J$  = 7.5 Hz, 1H,  $H_{10}$ ), 6.73 (d,  $J$  = 9.2 Hz, 1H,  $H_5$ ), 5.28 (s, 2H,  $CH_2$ ), 5.22 (s, 2H,  $CH_2$ ), 3.65 (s, 3H,  $OCH_3$ ), 3.50 (s, 3H,  $OCH_3$ ), 2.38 (s, 3H,  $CH_3$ );  $^{13}C$  NMR (175 MHz,  $CDCl_3$ )  $\delta$  192.72, 158.63, 156.38, 145.18, 138.73, 134.62, 134.02, 131.73, 129.21, 128.93, 126.12, 125.92, 119.97, 116.13, 106.06, 98.04, 94.63, 57.31, 56.53, 21.37; HRMS (EI)  $m/z$  calcd for  $C_{20}H_{22}O_6(M^+)$  359.1416, found 359.1492.

*(E)*-1-(2-hydroxy-3,4-bis(methoxymethoxy)phenyl)-3-(4-methoxyphenyl)prop-2-en-1-one (**13b**)

Synthesis was completed according to the general synthetic procedure mentioned above. The product was isolated by silica gel chromatography using ethyl acetate/petroleum ether (1:5) as yellow powder with 68.4 % yield; mp 107 – 109 °C;  $^1H$  NMR (400 MHz, Acetone- $d_6$ )  $\delta$  13.59 (s, 1H, OH), 8.01 (d,  $J$  = 9.2 Hz, 1H,  $H_6$ ), 7.89 (d,  $J$  = 15.4 Hz, 1H,  $H_\beta$ ), 7.85 – 7.79 (m, 3H,  $H_\alpha$ ,  $H_8$ ,  $H_{12}$ ), 7.03 (s, 1H,  $H_9$ ), 7.01 (s, 1H,  $H_{11}$ ), 6.80 (d,  $J$  = 9.1 Hz, 1H,  $H_5$ ), 5.35 (s, 2H,  $CH_2$ ), 5.15 (s, 2H,  $CH_2$ ), 3.87 (s, 3H,  $OCH_3$ ), 3.60 (s, 3H,  $OCH_3$ ), 3.49 (s, 3H,  $OCH_3$ );  $^{13}C$  NMR (175 MHz,  $CDCl_3$ )  $\delta$  192.67, 161.96, 158.59, 156.20, 144.84, 134.02, 130.50, 127.42, 125.94, 117.68, 116.19, 114.51, 105.97, 98.04, 94.63, 57.30, 56.52, 55.47; HRMS (EI)  $m/z$  calcd for  $C_{20}H_{22}O_7(M^+)$  375.1366, found 375.1434.

*(E)*-3-(3-chlorophenyl)-1-(2-hydroxy-3,4-bis(methoxymethoxy)phenyl)prop-2-en-1-one (**13c**)

Synthesis was completed according to the general synthetic procedure mentioned above. The product was isolated by silica gel chromatography using ethyl acetate/petroleum ether (1:5) as yellow powder with 65.0 % yield; mp 85 – 87 °C;  $^1H$  NMR (400 MHz,  $CDCl_3$ )  $\delta$  13.18 (s, 1H, OH), 7.79 (d,  $J$  = 15.5 Hz, 1H,  $H_\beta$ ), 7.64 (d,  $J$  = 9.2 Hz, 1H,  $H_6$ ), 7.62 (s, 1H,  $H_8$ ), 7.54 (d,  $J$  = 15.5 Hz, 1H,  $H_\alpha$ ), 7.49 (d,  $J$  = 7.0 Hz, 1H,  $H_{12}$ ), 7.41 – 7.32 (m, 2H,  $H_{10}$ ,  $H_{11}$ ), 6.76 (d,  $J$  = 9.2 Hz, 1H,  $H_5$ ), 5.30 (s, 2H,  $CH_2$ ), 5.22 (s, 2H,  $CH_2$ ), 3.66 (s, 3H,  $OCH_3$ ), 3.52 (s, 3H,  $OCH_3$ );  $^{13}C$  NMR (100 MHz,  $CDCl_3$ )  $\delta$  196.65, 161.94, 160.53, 146.71, 140.83, 138.60, 137.51, 134.09, 134.03, 131.91,

130.87, 130.66, 125.80, 119.64, 109.96, 101.66, 98.34, 60.13, 59.40; HRMS (EI)  $m/z$  calcd for  $C_{19}H_{19}ClO_6$  ( $M^+$ ) 379.0870, found 379.0940.

*(E)*-3-(*m*-tolyl)-1-(2,3,4-trihydroxyphenyl)prop-2-en-1-one (**14a**)

Synthesis was completed according to the general synthetic procedure mentioned above. The product was recrystallized using ethyl acetate/petroleum ether (1:1) as yellow powder with 89.6 % yield; mp 153 – 155 °C;  $^1H$  NMR (400 MHz, Acetone- $d_6$ )  $\delta$  13.53 (s, 1H, OH), 7.93 (d,  $J$  = 15.5 Hz, 1H,  $H_\beta$ ), 7.84 (d,  $J$  = 15.5 Hz, 1H,  $H_\alpha$ ), 7.73 (d,  $J$  = 8.9 Hz, 1H,  $H_6$ ), 7.68 (s, 1H,  $H_8$ ), 7.62 (d,  $J$  = 7.6 Hz, 1H,  $H_{12}$ ), 7.33 (t,  $J$  = 7.6 Hz, 1H,  $H_{11}$ ), 7.26 (d,  $J$  = 7.5 Hz, 1H,  $H_{10}$ ), 6.53 (d,  $J$  = 8.9 Hz, 1H,  $H_5$ ), 2.37 (s, 3H,  $CH_3$ );  $^{13}C$  NMR (175 MHz, Acetone- $d_6$ )  $\delta$  192.51, 153.44, 152.04, 144.12, 138.58, 134.95, 132.41, 131.40, 129.26, 128.85, 126.15, 122.58, 120.55, 113.86, 107.59, 20.42; HRMS (EI)  $m/z$  calcd for  $C_{16}H_{14}O_4$  ( $M^+$ ) 271.0892, found 271.0951.

*(E)*-3-(4-methoxyphenyl)-1-(2,3,4-trihydroxyphenyl)prop-2-en-1-one (**14b**)

Synthesis was completed according to the general synthetic procedure mentioned above. The product was recrystallized using ethyl acetate/petroleum ether (1:1) as yellow brown powder with 88.3 % yield; mp 151 – 153 °C;  $^1H$  NMR (400 MHz,  $CDCl_3$ )  $\delta$  13.62 (s, 1H, OH), 7.87 (d,  $J$  = 15.4 Hz, 1H,  $H_\beta$ ), 7.62 (d,  $J$  = 8.7 Hz, 2H,  $H_8$ ,  $H_{12}$ ), 7.47 (d,  $J$  = 8.9 Hz, 1H,  $H_6$ ), 7.39 (d,  $J$  = 15.4, 1H,  $H_\alpha$ ), 6.95 (d,  $J$  = 8.7 Hz, 2H,  $H_9$ ,  $H_{11}$ ), 6.57 (d,  $J$  = 8.9 Hz, 1H,  $H_5$ ), 3.87 (s, 3H,  $OCH_3$ );  $^{13}C$  NMR (175 MHz, MeOD)  $\delta$  192.60, 161.94, 153.04, 151.96, 143.72, 132.37, 130.20, 127.51, 121.97, 117.80, 114.07, 113.76, 107.20, 54.49; HRMS (EI)  $m/z$  calcd for  $C_{16}H_{14}O_5$  ( $M^+$ ) 287.0841, found 287.0917

*(E)*-3-(3-chlorophenyl)-1-(2,3,4-trihydroxyphenyl)prop-2-en-1-one (**14c**)

Synthesis was completed according to the general synthetic procedure mentioned above. The product was recrystallized using ethyl acetate/petroleum ether (1:1) as yellow powder with 88.4 % yield; mp 180 – 182 °C;  $^1H$  NMR (400 MHz, MeOD)  $\delta$  7.85 – 7.72 (m, 3H,  $H_\alpha$ ,  $H_\beta$ ,  $H_8$ ), 7.66– 7.63 (m, 1H,  $H_{12}$ ), 7.59 (d,  $J$  = 8.9 Hz, 1H,  $H_6$ ), 7.41 (d,  $J$  = 5.0 Hz, 2H,  $H_{10}$ ,  $H_{11}$ ), 6.49 (d,  $J$  = 8.9 Hz, 1H,  $H_5$ );  $^{13}C$  NMR (175 MHz, MeOD)  $\delta$  192.20, 153.11, 152.44, 141.77, 137.05, 134.62, 132.38, 130.11, 129.84, 127.86, 126.67, 122.33, 122.15, 113.68, 107.40; HRMS (EI)  $m/z$  calcd for  $C_{15}H_{11}ClO_4$  ( $M^+$ ) 291.0346, found 291.0569.

### Inhibition of self-mediated $A\beta_{1-42}$ aggregation assay

$A\beta_{1-42}$  protein was pretreated with 1,1,1,3,3,3-hexafluoro-2-propanol (HFIP) and was dissolved in DMSO as a stock solution of 1 mM. Experiments were performed by incubating the  $A\beta_{1-42}$  protein in 10 mM phosphate buffer (pH 7.4) containing 100 mM NaCl at 37 °C for 7 days at 25  $\mu$ M with or without inhibitors (25  $\mu$ M,  $A\beta$ /inhibitor = 1/1). Blanks containing the tested inhibitors were also prepared and tested. After incubation, samples were diluted to a final volume of 2.0 mL with 50 mM glycine-NaOH buffer (pH 8.0) containing 5  $\mu$ M thioflavin T. Measurement of fluorescence intensity was carried out using fluorescence microplate reader (spectra MAX GeminiXS, Molecular Devices) on a 96-well plate (Greiner bio-one, Germany) ( $\lambda_{ex}$ =440 nm;  $\lambda_{em}$ =485 nm). Percentage inhibition of aggregation was calculated using the formula  $(1-IF_i/IF_c) \times 100$  % in which  $IF_i$  and  $IF_c$  are the fluorescence intensities obtained in the presence and absence of inhibitors after subtracting the background, respectively. Each measurement was run in triplicate.

### Cell culture

SH-SY5Y cell line (human neuroblastoma cells) was cultured in DMEM/F12 media with 10 % fetal bovine serum (FBS), 1 % non-essential amino acids and 1 % penicillin/streptomycin in a 37 °C incubator containing 5 % CO<sub>2</sub> humidified atmosphere. HEK-293 cells were cultured in DMEM media with 10 % FBS, 1 % penicillin/streptomycin and 1 mM sodium pyruvate under the same environment with SH-SY5Y. The culture media were changed every three days.

### Determination of neurotoxicity in SH-SY5Y cells

SH-SY5Y cells were seeded into 96-well plates at a density of  $2 \times 10^4$  cells/100  $\mu$ L/well. Cells were allowed to adhere for 24 h. To test the toxicity of the compounds, cells were treated with different concentrations of compounds for 24 h on the next day. Cell viability was determined using the CellTiter 96 Aqueous One Solution Assay (MTS assay; Promega) following the manufacturer's instruction. Absorbance at 490 nm was measured on a fluorescent microplate reader 4 hours later. The cell viability was directly proportional to the absorbance of each well and normalized by negative control group. Data are reported as the mean  $\pm$  standard deviation of at least three independent experiments.

### Determination of neuroprotective activities in SH-SY5Y cells

To measure the neuroprotective activities from A $\beta$  toxicity of the selected compounds, SH-SY5Y cells were seeded into 96-well plates at a density of  $2 \times 10^4$  cells/100  $\mu$ L/well. Cells were allowed to adhere for 24 h. A $\beta_{1-42}$  (10  $\mu$ M) was then added to the wells after addition of different concentrations of compounds. After 48 h, cell viability was determined using MTS assay as mentioned above. Data are reported as the mean  $\pm$  standard deviation of at least three independent experiments.

### ADMET prediction

ADMET prediction was carried out using the Discovery Studio 3.1 (DS). The three-dimensional structures of the selected compounds were constructed using ChemBio3D Ultra 12.0 software. The ADMET properties of compounds was predicted using ADMET Tool in DS.

### Determination of ferroptosis inhibition activities in HEK-293 cells

HEK-293 cells (5000 cells in 100  $\mu$ L media) were seeded in a 96-well plate and incubated for 24 h. Ferroptosis was induced by (1*S*,3*R*)-RSL3 (500 nM) or erastin (10  $\mu$ M) after addition of different concentrations of compounds for 4 h. On the next day, cell viability was assessed using the CellTiter 96 Aqueous One Solution Assay (MTS assay; Promega) as mentioned above. Cell viability was calculated by normalizing the data to vehicle group. Data are reported as the mean  $\pm$  standard deviation of at least three independent experiments.

### Determination of cellular lipid peroxidation inhibition activities

SH-SY5Y ( $2 \times 10^4$  in 100  $\mu$ L media) cells were seeded in a 96-well plate and incubated for 24 h. On the next day, the cells were incubated with the tested compounds and A $\beta_{1-42}$  (20  $\mu$ M) or RSL3 (500 nM) for another 48 h or 24 h, respectively. Cells were treated with BODIPY-C11<sup>581/591</sup> (1  $\mu$ M) and incubated at 37 °C in dark for 30 minutes. Cells were then analyzed by flow cytometry ( $\lambda_{ex}$  =

488 nm;  $\lambda_{em} = 525 \pm 25$  nm). Cells treated with diethylmaleate (DEM, 1 mM) alone but no A $\beta_{1-42}$  protein or RSL3 was used as a positive control. Cells treated with A $\beta_{1-42}$  or RSL3 alone but no test compounds were used as positive control as well. Cells from untreated cultures were used as negative control. Data were collected 10,000 events per sample and reported as the mean  $\pm$  standard deviation of at least three independent experiments.

### Conflicts of Interest

There are no conflicts to declare.

### Acknowledgements

We acknowledge the support by the Fund of Innovation Center of Radiation Application, China (KFZC2018040208), National Key Scientific Instrument and Equipment Project of the Ministry of Science and Technology of China (2013YQ03059514) and the Beijing Institute of Technology Research Fund Program for Young Scholars. We acknowledge Prof. Hong Qing at Beijing Institute of Technology for helpful discussions.

### Reference

- [1] B. De Strooper, E. Karran, The cellular phase of alzheimer's disease, *Cell*, 164 (2016) 603-615.
- [2] E. McDade, R.J. Bateman, Stop alzheimer's before it starts, *Nature*, 547 (2017) 153-155.
- [3] A. Wimo, L. Jonsson, J. Bond, M. Prince, B. Winblad, A.D. Int, The worldwide economic impact of dementia 2010, *Alzheimers & Dementia*, 9 (2013) 1-11.
- [4] J. Rodda, J. Carter, Cholinesterase inhibitors and memantine for symptomatic treatment of dementia, *Br. Med. J.*, 344 (2012) 43-49.
- [5] E. Viayna, I. Sola, M. Bartolini, S.A. De, C. Tapiarajas, F.G. Serrano, R. Sabaté, J. Juárezjiménez, B. Pérez, F.J. Luque, Synthesis and multitarget biological profiling of a novel family of rhein derivatives as disease-modifying anti-alzheimer agents, *J. Med. Chem.*, 57 (2014) 2549-2567.
- [6] E. Karran, M. Mercken, B. De Strooper, The amyloid cascade hypothesis for alzheimer's disease: An appraisal for the development of therapeutics, *Nat. Rev. Drug Discovery*, 10 (2011) 698-712.
- [7] J. Hardy, D.J. Selkoe, Medicine - the amyloid hypothesis of alzheimer's disease: Progress and problems on the road to therapeutics, *Science*, 297 (2002) 353-356.
- [8] D.J. Selkoe, Alzheimer's disease: Genes, proteins, and therapy, *Physiol. Rev.*, 81 (2001) 741-766.
- [9] W.S. Hambright, R.S. Fonseca, L.J. Chen, R. Na, Q.T. Ran, Ablation of ferroptosis regulator glutathione peroxidase 4 in forebrain neurons promotes cognitive impairment and neurodegeneration, *Redox Biol.*, 12 (2017) 8-17.
- [10] Y.H. Zhang, D.W. Wang, S.F. Xu, S. Zhang, Y.G. Fan, Y.Y. Yang, S.Q. Guo, S. Wang, T. Guo, Z.Y. Wang, C. Guo, Alpha-lipoic acid improves abnormal behavior by mitigation of oxidative stress, inflammation, ferroptosis, and tauopathy in p301s tau transgenic mice, *Redox Biol.*, 14 (2018) 535-548.
- [11] S.J. Dixon, K.M. Lemberg, M.R. Lamprecht, R. Skouta, E.M. Zaitsev, C.E. Gleason, D.N. Patel, A.J. Bauer, A.M. Cantley, W.S. Yang, B. Morrison, B.R. Stockwell, Ferroptosis: An iron-dependent form of nonapoptotic cell death, *Cell*, 149 (2012) 1060-1072.

- [12] J.P.F. Angeli, R. Shah, D.A. Pratt, M. Conrad, Ferroptosis inhibition: Mechanisms and opportunities, *Trends Pharmacol. Sci.*, 38 (2017) 489-498.
- [13] B.R. Stockwell, J.P.F. Angeli, H. Bayir, A.I. Bush, M. Conrad, S.J. Dixon, S. Fulda, S. Gascon, S.K. Hatzios, V.E. Kagan, K. Noel, X.J. Jiang, A. Linkermann, M.E. Murphy, M. Overholtzer, A. Oyagi, G.C. Pagnussat, J. Park, Q. Ran, C.S. Rosenfeld, K. Salnikow, D.L. Tang, F.M. Torti, S.V. Torti, S. Toyokuni, K.A. Woerpel, D.D. Zhang, Ferroptosis: A regulated cell death nexus linking metabolism, redox biology, and disease, *Cell*, 171 (2017) 273-285.
- [14] E.D. Hall, Novel inhibitors of iron-dependent lipid-peroxidation for neurodegenerative disorders, *Ann. Neurol.*, 32 (1992) S137-S142.
- [15] B.R. Cardoso, D.J. Hare, M. Lind, C.A. McLean, I. Volitakis, S.M. Laws, C.L. Masters, A.I. Bush, B.R. Roberts, The apoe epsilon 4 allele is associated with lower selenium levels in the brain: Implications for alzheimer's disease, *ACS Chem. Neurosci.*, 8 (2017) 1459-1464.
- [16] L.J. Chen, W.S. Hambright, R. Na, Q.T. Ran, Ablation of the ferroptosis inhibitor glutathione peroxidase 4 in neurons results in rapid motor neuron degeneration and paralysis, *J. Biol. Chem.*, 290 (2015) 28097-28106.
- [17] W.R. Markesbery, Oxidative stress hypothesis in alzheimer's disease, *Free Radic. Biol. Med.*, 23 (1997) 134-147.
- [18] F. Gu, M.J. Zhu, J.T. Shi, Y.H. Hu, Z. Zhao, Enhanced oxidative stress is an early event during development of alzheimer-like pathologies in presenilin conditional knock-out mice, *Neurosci. Lett.*, 440 (2008) 44-48.
- [19] L.J. Chen, R. Na, M.J. Gu, A. Richardson, Q. Ran, Lipid peroxidation up-regulates bace1 expression in vivo: A possible early event of amyloidogenesis in alzheimer's disease, *J. Neurochem.*, 107 (2008) 197-207.
- [20] D.A. Butterfield, A. Castegna, C.M. Lauderback, J. Drake, Evidence that amyloid beta-peptide-induced lipid peroxidation and its sequelae in alzheimer's disease brain contribute to neuronal death, *Neurobiol. Aging*, 23 (2002) 655-664.
- [21] P. Meena, V. Nemaish, M. Khatri, A. Manral, P.M. Luthra, M. Tiwari, Synthesis, biological evaluation and molecular docking study of novel piperidine and piperazine derivatives as multi-targeted agents to treat alzheimer's disease, *Biorg. Med. Chem.*, 23 (2015) 1135-1148.
- [22] R. Sultana, M. Perluigi, D.A. Butterfield, Lipid peroxidation triggers neurodegeneration: A redox proteomics view into the alzheimer disease brain, *Free Radic. Biol. Med.*, 62 (2013) 157-169.
- [23] N. Guzior, M. Bajda, M. Skrok, K. Kurpiewska, K. Lewinski, B. Brus, A. Pislak, J. Kos, S. Gobec, B. Malawska, Development of multifunctional, heterodimeric isoindoline-1,3-dione derivatives as cholinesterase and beta-amyloid aggregation inhibitors with neuroprotective properties, *Eur. J. Med. Chem.*, 92 (2015) 738-749.
- [24] L.F. Pan, X.B. Wang, S.S. Xie, S.Y. Li, L.Y. Kong, Multitarget-directed resveratrol derivatives: Anti-cholinesterases, anti-beta-amyloid aggregation and monoamine oxidase inhibition properties against alzheimer's disease, *Medchemcomm*, 5 (2014) 609-616.
- [25] C. Ramassamy, Emerging role of polyphenolic compounds in the treatment of neurodegenerative diseases: A review of their intracellular targets, *Eur. J. Pharmacol.*, 545 (2006) 51-64.
- [26] B.M. Rezk, G.R.M.M. Haenen, W.J.F. van der Vijgh, A. Bast, The antioxidant activity of phloretin: The disclosure of a new antioxidant pharmacophore in flavonoids, *Biochem. Biophys.*

Res. Commun., 295 (2002) 9-13.

- [27] Y.S. Li, K. Matsunaga, R. Kato, Y. Ohizumi, Verbenachalcone, a novel dimeric dihydrochalcone with potentiating activity on nerve growth factor-action from verbena littoralis, *J. Nat. Prod.*, 64 (2001) 806-808.
- [28] N. Li, Z.J. Ma, M.J. Li, Y.C. Xing, Y. Hou, Natural potential therapeutic agents of neurodegenerative diseases from the traditional herbal medicine chinese dragon's blood, *J. Ethnopharmacol.*, 152 (2014) 508-521.
- [29] J.H. Liang, L. Yang, S. Wu, S.S. Liu, M. Cushman, J. Tian, N.M. Li, Q.H. Yang, H.A. Zhang, Y.J. Qiu, L. Xiang, C.X. Ma, X.M. Li, H. Qing, Discovery of efficient stimulators for adult hippocampal neurogenesis based on scaffolds in dragon's blood, *Eur. J. Med. Chem.*, 136 (2017) 382-392.
- [30] H. Levine, Thioflavine-t interaction with synthetic alzheimers-disease beta-amyloid peptides - detection of amyloid aggregation in solution, *Protein Sci.*, 2 (1993) 404-410.
- [31] E. Hofmann, J. Webster, T. Do, R. Kline, L. Snider, Q. Hauser, G. Higginbottom, A. Campbell, L.L. Ma, S. Paula, Hydroxylated chalcones with dual properties: Xanthine oxidase inhibitors and radical scavengers, *Biorg. Med. Chem.*, 24 (2016) 578-587.
- [32] G.C. Wang, F. Peng, D. Cao, Z. Yang, X.L. Han, J. Liu, W.S. Wu, L. He, L. Ma, J.Y. Chen, Y. Sang, M.L. Xiang, A.H. Peng, Y.Q. Wei, L.J. Chen, Design, synthesis and biological evaluation of millepachine derivatives as a new class of tubulin polymerization inhibitors, *Biorg. Med. Chem.*, 21 (2013) 6844-6854.
- [33] X.K. Li, H. Wang, Z.Y. Lu, X.Y. Zheng, W. Ni, J. Zhu, Y. Fu, F.L. Lian, N.X. Zhang, J. Li, H.Y. Zhang, F. Mao, Development of multifunctional pyrimidinylthiourea derivatives as potential anti-alzheimer agents, *J. Med. Chem.*, 59 (2016) 8326-8344.
- [34] H. Kroth, N. Sreenivasachary, A. Hamel, P. Benderitter, Y. Varisco, V. Giriens, P. Paganetti, W. Froestl, A. Pfeifer, A. Muhs, Synthesis and structure-activity relationship of 2,6-disubstituted pyridine derivatives as inhibitors of beta-amyloid-42 aggregation, *Biorg. Med. Chem. Lett.*, 26 (2016) 3330-3335.
- [35] J.A. Carver, P.J. Duggan, H. Ecroyd, Y.Q. Liu, A.G. Meyer, C.E. Tranberg, Carboxymethylated-kappa-casein: A convenient tool for the identification of polyphenolic inhibitors of amyloid fibril formation, *Biorg. Med. Chem.*, 18 (2010) 222-228.
- [36] M. Convertino, R. Pellarin, M. Catto, A. Carotti, A. Caflisch, 9,10-anthraquinone hinders beta-aggregation: How does a small molecule interfere with a beta-peptide amyloid fibrillation?, *Protein Sci.*, 18 (2009) 792-800.
- [37] J.F.S. Carvalho, M.M.C. Silva, J.N. Moreira, S. Simoes, M.L.S.E. Melo, Selective cytotoxicity of oxysterols through structural modulation on rings a and b. Synthesis, in vitro evaluation, and sar, *J. Med. Chem.*, 54 (2011) 6375-6393.
- [38] Q.I. Churches, J. Caine, K. Cavanagh, V.C. Epa, L. Waddington, C.E. Tranberg, A.G. Meyer, J.N. Varghese, V. Streltsov, P.J. Duggan, Naturally occurring polyphenolic inhibitors of amyloid beta aggregation, *Biorg. Med. Chem. Lett.*, 24 (2014) 3108-3112.
- [39] V.L.N. Ngoungoure, J. Schluesener, P.F. Moundipa, H. Schluesener, Natural polyphenols binding to amyloid: A broad class of compounds to treat different human amyloid diseases, *Mol. Nutr. Food. Res.*, 59 (2015) 8-20.
- [40] Z.M. Wang, P. Cai, Q.H. Liu, D.Q. Xu, X.L. Yang, J.J. Wu, L.Y. Kong, X.B. Wang, Rational modification of donepezil as multifunctional acetylcholinesterase inhibitors for the treatment of

alzheimer's disease, *Eur. J. Med. Chem.*, 123 (2016) 282-297.

[41] O. Zilka, R. Shah, B. Li, J.P.F. Angeli, M. Griesser, M. Conrad, D.A. Pratt, On the mechanism of cytoprotection by ferrostatin-1 and liproxstatin-1 and the role of lipid peroxidation in ferroptotic cell death, *Acs. Cent. Sci.*, 3 (2017) 232-243.

[42] S. Ayton, A.I. Bush, Iron and ferroptosis in the pathogenesis of alzheimer's disease, *Free Radic. Biol. Med.*, 120 (2018) S8-S8.

[43] D.A. Pratt, K.A. Tallman, N.A. Porter, Free radical oxidation of polyunsaturated lipids: New mechanistic insights and the development of peroxy radical clocks, *Acc. Chem. Res.*, 44 (2011) 458-467.

[44] Y.M.A. Naguib, A fluorometric method for measurement of peroxy radical scavenging activities of lipophilic antioxidants, *Anal. Biochem.*, 265 (1998) 290-298.

[45] W.S. Yang, B.R. Stockwell, Synthetic lethal screening identifies compounds activating iron-dependent, nonapoptotic cell death in oncogenic-ras-harboring cancer cells, *Chem. Biol.*, 15 (2008) 234-245.

[46] A. Seiler, M. Schneider, H. Forster, S. Roth, E.K. Wirth, C. Culmsee, N. Plesnila, E. Kremmer, O. Radmark, W. Wurst, G.W. Bornkamm, U. Schweizer, M. Conrad, Glutathione peroxidase 4 senses and translates oxidative stress into 12/15-lipoxygenase dependent- and aif-mediated cell death, *Cell Meta.*, 8 (2008) 237-248.

## Highlights

- Hydroxylated chalcones were synthesized as dual-functional inhibitors.
- Chalcones **14a-c** inhibited amyloid- $\beta$  aggregation at micromolar concentrations.
- Chalcones **14a-c** protected neural cells against A $\beta$  aggregation induced toxicity.
- Chalcones **14a-c** protected cells from ferroptosis at micromolar concentrations.